IEEE Access
Multidisciplinary | Rapid Review | Open Access Journal

Received 3 December 2023, accepted 30 December 2023, date of publication 2 January 2024,
date of current version 9 January 2024.

Digital Object Identifier 10.1109/ACCESS.2023.3349294

RESEARCH ARTICLE

Design of a Parallel All-DC Wind Power System With Turbine-Side Boost Based on a New DC Conversion

HAIYANG HAN[1], ZHANLONG LI[2], HAIYUN WANG[1], QITA FENG[2], RUI GUO[2], ZHIQIAN YANG[2], AND XIANGPING LIU[2]

[1]College of Electrical Engineering, Xinjiang University, Ürümqi 830017, China
[2]Beijing Goldwind Science and Creation Wind Power Equipment Company Ltd., Beijing 100176, China

Corresponding author: Haiyun Wang (why@xju.edu.cn)

This work was supported in part by the National Key Research and Development Program of China under Grant 2021YFB1507005.

ABSTRACT All-DC wind power system is one of the important directions of wind power development in the future, and its safe and reliable topology and stable control strategy are the key to the stable operation of the system. In order to solve the problems of poor control flexibility, difficulty of self-starting and low reliability of DC fault crossing in the current all-DC wind farm, this paper presented a topological structure of the parallel all-DC wind power system with turbine-side boost based on a new DC conversion. Based on the dynamic connection mode that each bridge arm of the new DC converter was charged in parallel on the low voltage side and discharged in series on the high voltage side, this paper designed the control strategy of the all-DC wind farm and analysed the operation mode of the all-DC wind farm in the steady state operation stage, the self-starting stage and the DC fault crossing period. Based on PSCAD/EMTDC, the simulation model of the parallel all-DC wind power system with turbine-side boost based on a new DC converter was established. Through the simulation of all-DC wind farm under normal operating conditions, such as steady state and dynamic operation, and fault conditions, such as dynamic cut-in and cut-out of faulty wind turbine and short circuit of DC bus, it was verified that the topology structure of the proposed parallel all-DC wind power system with turbine-side boost based on a new DC converter could improve the control flexibility, reduce the difficulty of self-starting, and ensure the high reliability of DC fault crossing under the premise of feasibility.

INDEX TERMS All-dc wind power system, new dc converter, parallel, topological structure, control strategy.

I. INTRODUCTION

With the further development of renewable energy power generation technology, the wind power industry is in a period of vigorous development, and the scale of wind power base continues to expand [1], [2], [3]. In order to effectively solve the problems of harmonic resonance [4], [5], [6] and overvoltage caused by reactive power [7] existing in the wind power system and realize the efficient transmission of electric energy [8], the advantages of the all-DC wind power system scheme that adopts DC collection and DC transmission are gradually obvious [9], [10].

The topology of all-DC wind power system can be divided into series [11], [12] and parallel [13], [14] networks according to the different modes of electric energy collection in wind farms. Due to the strong coupling characteristics among the DC wind turbines in the series all-DC wind power system, the outlet voltage and output power of the DC wind turbines interact with each other, and the phenomenon of wind curtailment occurs during voltage limit period of DC wind turbine [15], [16], which not only greatly improves the control difficulty of the topology structure [17], but also restricts the realization of DC series wind farm [18]. However, the parallel all-DC wind

The associate editor coordinating the review of this manuscript and approving it for publication was Xueguang Zhang.

© 2024 The Authors. This work is licensed under a Creative Commons Attribution-NonCommercial-NoDerivatives 4.0 License.
For more information, see https://creativecommons.org/licenses/by-nc-nd/4.0/

power system has a flexible structure due to the fact that the DC wind turbines are in parallel with each other, which makes the topology of the topology more scalable, more conducive to the decentralized control of the DC wind turbines, and the coupling of electrical parameters is smaller than that of the series all-DC wind power system [19]. Therefore, it has the characteristics of high reliability and easy implementation to use the parallel all-DC wind power system topology to construct all-DC wind power system.

The topology structure of the parallel all-DC wind power system can be divided into one cluster step-up type, two step-ups type and turbine step-up type according to the position and number of DC step-up converters [20], [21]. The one cluster step-up topology will directly convert the low voltage electric energy collected by the wind farm to high voltage through one boost. Although the loss caused by the one cluster step-up topology in the step-up process is relatively small [22], the maximum generator-side line voltage of the wind turbine is only 5kV [23], and the topology requires a high capacity of a single DC step-up converter [24], [25], which leads to the high energy loss of this topology in the process of DC collecting [26] and has great difficulty in engineering implementation of this topology. Although the two step-ups topology reduces the ratio of DC step-up converter, the energy loss in the process of electric energy collection [19] through the two step-ups way, the topology causes a large energy loss in the step-up process [14], which greatly affects the efficiency of energy transmission [22]. In the turbine step-up topology not only reduces the step-up loss and energy loss in the process of power collection by directly realizing high ratio voltage conversion at the outlet of DC wind turbine [22], but also realizes independent control of turbine-side voltage and power through turbine-side DC step-up converter [19]. According to the comparative analysis of the above studies, in order to realize the efficient operation of the all-DC wind power system, the parallel all-DC wind power system topology with turbine-side boost has more obvious advantages.

The topology of DC/DC converter and the operation control of wind power system are very important in order to realize the safe and stable operation of the parallel all-DC wind power system. In the topology of DC converter [27], [28] applied to wind power system, [29] proposes a kind of DC converter based on IPOS, but the topology has the problem of voltage balancing or current balancing due to the direct series or parallel connection of multiple subunits; [30], [31], [32] propose an M2DC converter based on MMC, but due to the large number of modules in the topology and the existence of intermediate frequency transformer, the switching loss and manufacturing cost are increased; [33] proposes a DC autotransformer with fault isolation function, but the system takes a long time to restart after the DC fault is cleared; [34] proposes a modular hybrid cascade DC/DC converter with bi-directional power transmission capability, but this topology only has unidirectional fault blocking capability and cannot block short-circuit faults on the high-voltage side; [35] proposes a new topology of DC converter. However, due to the facts that the energy flow in this topology cannot be reversed by using diodes at the input and output sides, and the DC voltage on the low voltage side is directly set through the voltage source, and the voltage control on the low voltage side cannot be realized, the application of this topology in the all-DC wind power system needs further study.

In the research of the operation characteristics and control strategy of the parallel all-DC wind power system, [36] proposes a grid-connected structure of the parallel all-DC wind power system with turbine-side boost based on MIDC DC converter with high efficiency and high energy density. However, the MPPT control of PMSG output power in the wind farm control strategy only considers the small difference in wind speed between wind turbine units; [37] proposes a two step-ups parallel all-DC wind power system structure. However the ideal controlled current source is used to replace the wind turbine, which leads the actual characteristics of the wind turbine are not fully considered; [38] proposes a topology structure of one cluster step-up parallel all-DC wind power system based on single-phase full-bridge DC converter. However, the single-phase full-bridge DC converter used in this system cannot realize energy return, which leads the wind power system does not have the ability of self-starting; [39] proposes a power-reduction control strategy (PRCS), which improves the transient performance of offshore wind farms when the voltage of onshore AC grid drops. However, the DC bus voltage of the wind turbine rises too high during the fault period, which may exceed the capacitance withstand voltage value; [14] proposes a fault protection method for DC wind farms based on bipolar transmission lines, but only the offshore converter is blocked when the fault occurs, and the capacitor is still discharged to the fault point

In view of the above problems existing in the current all-DC wind power system, this paper proposes a parallel all-DC wind power system topology with turbine-side boost by applying a new DC converter to the all-DC wind power farm. By improving the topology structure of the new DC converter and putting forward a new control strategy of the DC converter, the application capability of the DC converter in all DC wind farms is improved, and the problems of poor control flexibility, difficult self-starting and low reliability of fault crossing are effectively solved in all-DC wind farms. The rest of this paper is organized as follows: In Section II, the topology, steady-state operation characteristics, and self-starting of the parallel all-DC wind power generation system are analysed. The III Section introduces the steady-state control strategy of the parallel all-DC wind power generation system in detail. In IV Section, the fault handling strategy of the parallel all DC wind power system is proposed. In V Section, the operation advantages of the proposed topology are compared and analyzed. In VI Section, a simulation study is carried out to verify the effectiveness

of the proposed parallel all-DC wind power system topology and its control strategy. Finally, the VII Section gives the conclusion.

II. PARALLEL ALL-DC WIND POWER SYSTEM

A. TOPOLOGY OF THE PARALLEL ALL-DC WIND POWER SYSTEM

This paper proposes a topology structure of the parallel all-DC wind power system with turbine-side boost based on a new DC conversion. The system scheme is shown in Fig. 1. Each DCWT in the wind farm first converts the AC low voltage from the generator into DC low voltage through the generator-side AC/DC converter, and then converts the DC low voltage into DC high voltage through the DC converter, and finally outputs the DC electric energy. The power is collected on the HVDC busbar by connecting multiple DCWT units after boost conversion in parallel, then is transmitted to the specified MMC converter station through the HVDC transmission line. Finally, it is integrated into the AC grid through the AC transformer to realize the stable transmission of energy.

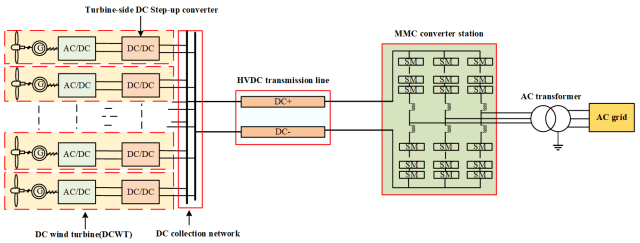

FIGURE 1. The parallel all-DC wind power system.

In Fig. 1, DC wind turbine (DCWT) after step-up conversion is the basic unit of the parallel all-DC wind power generation system, and its topology is shown in Fig. 2.

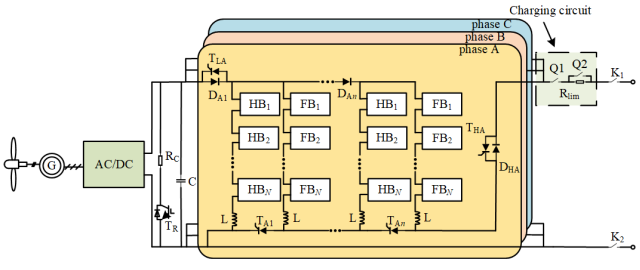

FIGURE 2. DCWT topology based on DC step-up conversion.

DCWT based on DC step-up conversion is mainly composed of fan blade, permanent magnet synchronous generator, AC/DC converter, energy dissipation circuit (T_R, R_C), support capacitor C, new DC converter, charging circuit (R_{lim}, Q_1, and Q_2), isolation switch (K_1, K_2.) and so on.

In Fig. 2, the AC/DC converter adopts a two-level voltage source converter, as shown in Fig. 3, where u_{as}, u_{bs}, and u_{cs} are the AC input voltage of the rectifier; U_L is the DC voltage output after being rectified on the machine side.

In order to ensure that the output voltage of DCWT can be stably transformed from low voltage to high voltage DC, a new non-isolated DC converter [35] is adopted in this paper. Based on this topology, by adding reverse thyristors to the input and output sides, the improved topology has the ability of energy reverse flow. The topology is shown in Fig. 4.

The topology consists of three phases (phase A, phase B, and phase C.) in parallel, each phase of the circuit structure is exactly the same. Each single-phase circuit contains n half-bridge arms, n full-bridge arms and n diode valves D_{ik} (i =A, B, and C; $k = 1, 2\ldots, n$.) and a diode valve D_{Hi} (i =A, B, and C.) directly connected with the high voltage DC port, n thyristor valves T_{ik} (i =A, B, and C; $k = 1, 2\ldots, n$), and the low voltage side and high voltage side reverse parallel thyristor T_{Li} and T_{Hi} (i =A, B, and C.) to control the reverse flow of energy. The full bridge arm is formed by N full bridge submodules FB and a bridge arm inductor L in series, and the half bridge arm is formed by N half bridge submodules HB and a bridge arm inductor L in series. In Fig. 4, U_L and I_L represent the voltage and current at the low-voltage DC port; U_H and I_H represent the voltage and current at the high-voltage DC port, respectively.

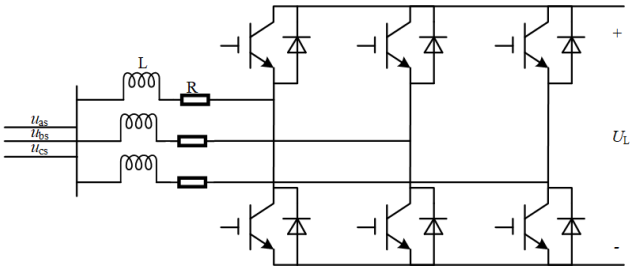

FIGURE 3. Voltage source type two level converter.

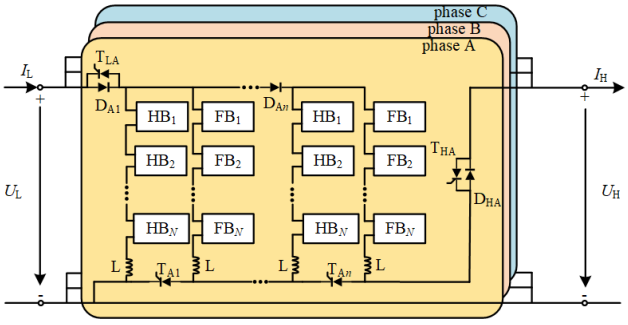

FIGURE 4. New DC converter.

In the existing [35], this topology cannot realize the reverse flow of energy and the voltage control of the low voltage side, which leads to the limitation of the application of this topology in the all-DC wind power system. Compared with the existing topology, this paper improves the topology of the new DC converter by parallelling reverse thyristors at the high and low voltage sides, which can lay a foundation for the realization of the energy reverse flow in this topology. In addition,

in order to improve the control coordination of the topology in the all-DC wind power system, this paper proposes a control strategy based on the number of control submodules and the voltage of the submodules (as shown in (2) of Section B of Part III), so that the topology can control the DC voltage on the low voltage side, which greatly improves the application of the topology in the all-DC wind power system. In addition, compared with the phase-shifted dual three-level DC/DC converters, phase-shifted multiple high-voltage M2DC converters [37], and the dual-active-bridge (DAB.) modular DC solid-state transformers (DCSST.) [40] currently used in all-DC wind farms, The topology structure of the DC converter used in this paper not only has the ability of energy reverse flow, but also avoids the circulation influence caused by the uneven voltage distribution of the DAB modular DCSST when energy reverse flow [41].

B. STEADY-STATE OPERATION OF THE PARALLEL ALL-DC WIND POWER SYSTEM

Since a parallel all-DC wind farm is formed by DCWT units in parallel, the operation mode of a single DCWT is the basis of stable operation of the whole wind farm. When the parallel all-DC wind power system is in steady operation, the wind energy is converted into mechanical energy by the fan blade in the DCWT, which is converted into AC electric energy (u_{sge}.) by the wind generator, and then converted into the low DC electric energy (U_{L}.) by the AC/DC converter. Finally, the low DC voltage is stepped up by the new DC converter and then output to the high voltage DC port to get the high voltage DC voltage U_{H}. The output energy of all DCWT inside the wind farm is collected in parallel, and then transmitted to the grid-side MMC by DC transmission. The AC energy (u_{sgr}.) is obtained through conversion, and finally it is transferred to the AC grid after transformer. The topology structure of the parallel all-DC wind power system during steady-state operation is shown in Fig. 5. At this time, the switching device in AC/DC converter is normally on and off, the isolation switch K_1 and K_2 are closed, the DC switch Q_1 and Q_2 are closed, the switch tube T_R in the energy dissipation circuit is disconnected, and all the power emitted by the wind turbine is transmitted to the high voltage DC port. The new DC converter steady-state operation mode is very important for the stable operation of DCWT. The new DC converter includes two operating modes in normal operation. Fig. 6 shows the parallel charging mode of the new DC converter. Fig. 7 shows the series discharge mode of the new DC converter.

In Fig. 6 and Fig. 7, U_{Chb} and U_{Cfb} are the capacitance voltage of half-bridge submodule and full-bridge submodule respectively; U_{HB} and U_{FB} are the output voltage of half bridge submodule and full bridge submodule respectively; I_{HB} and I_{FB} are half-bridge arm current and full-bridge arm current, respectively; R_{hb} and R_{fb} are the charging resistors of the half-bridge submodule and the full-bridge submodule, respectively.

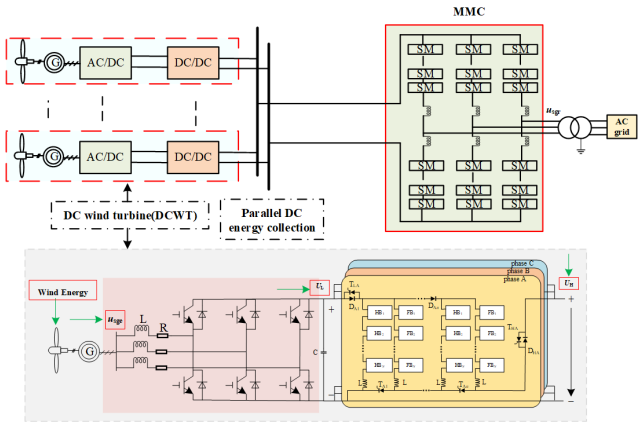

FIGURE 5. The topology structure of the parallel all-DC wind power system during steady-state operation.

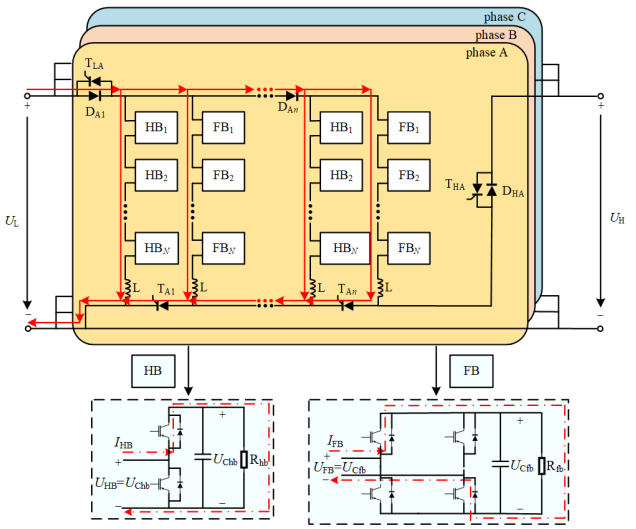

FIGURE 6. The parallel charging mode of the new DC converter.

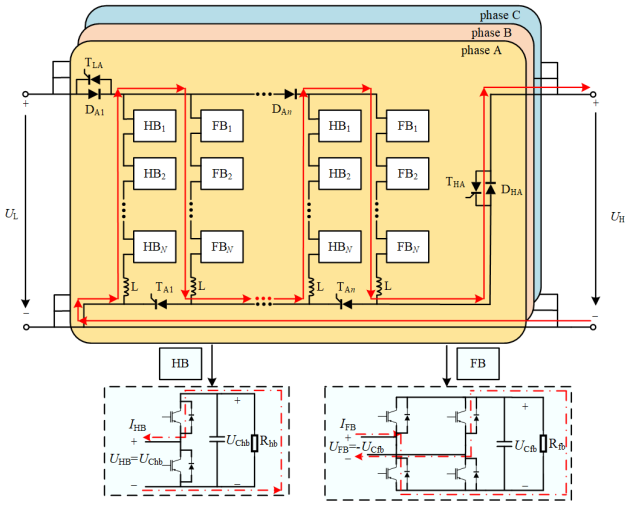

FIGURE 7. The series discharge mode of the new DC converter.

In steady-state operation, the new DC converter uses the series and parallel switching of submodule bridge arms to share the high current stress on the low voltage side and the high voltage stress on the high voltage side, and uses the

three-phase staggered operation of 120 degrees to offset the current fluctuations. Each phase circuit operates in two modes of parallel charging and series discharge through the nearest level modulation. In parallel charging mode, by controlling D_{ik}(i =A, B, and C; k=1, 2, …, n.) and T_{ik}(i =A, B, and C; k=1, 2, …, n.) on, and D_{Hi} (i =A, B, and C.) are forced to turn off. At this time, n half bridge arms and n full bridge arms are connected in parallel with the low voltage side, and the capacitor voltage of the submodules in each bridge arm is charged to the given value U_{Cref}, and the DC current I_L input on the low voltage side is evenly divided by all bridge arms. In series discharge mode, by controlling D_{ik}(i =A, B, and C; k=1, 2, …, n.) and T_{ik}(i =A, B, and C; k=1, 2, …, n.) off, and reversing the voltage of all full bridge submodules in n full bridge arms, n half bridge arms are connected to n full bridge arms in series and D_{Hi} (i =A, B, and C.) are forced to be switched on, so that all bridge arms are discharged in series to the high voltage side together, and stable high voltage DC is output. Finally, the energy inside DCWT can be transmitted stably and efficiently after DC converter. At this time, the DC current I_H output by the high voltage side is the same as the current of all the bridge arms.

Then n DCWT units based on the above operation mode are connected in parallel to form a all-DC wind farm, as shown in Fig. 8. U_{Lj} ($j = 1, 2\ldots, n.$) is the DC voltage output by the rectifier in the DCWT#j($j = 1, 2\ldots, n$); U_{Hj} and I_{Hj} ($j = 1, 2\ldots, n.$) are respectively the output voltage and output current of the new DC converter in the DCWT#j($j = 1, 2\ldots, n$). U_{HP} and I_{HP} are the voltage of the high voltage DC bus and the current of the high voltage DC transmission line.

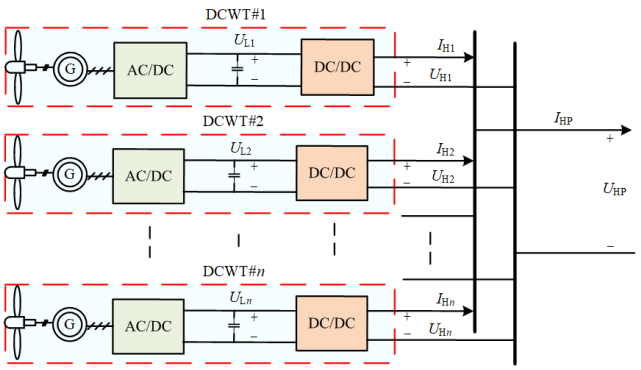

FIGURE 8. Parallel all-DC wind farm.

In Fig. 8, since the output voltage of each DCWT after step-up conversion reaches the level of DC transmission voltage, the DC bus voltage U_{HP} of the parallel all-DC wind farm can be expressed as:

$$U_{HP} = U_{HP}(j{=}1,2\ldots,n) \tag{1}$$

Set the output power of the DCWT#1 after step-up conversion as P_{Hj} ($j = 1, 2\ldots, n$), then the active power collected by the DC bus of the parallel all-DC wind farm and the current of the HVDC transmission line meet (2) and (3) respectively.

$$P_{HP} = \sum_{j=1}^{n} P_{Hj} = U_{HP} I_{HP} \tag{2}$$

$$I_{HP} = \sum_{j=1}^{n} I_{Hj} \tag{3}$$

In (2), P_{HP} is the active power collected by the DC bus of the parallel all-DC wind farm.

Since the outlet voltage of each DCWT after the step-up conversion is equal to the DC bus voltage, P_{Hj} can be expressed as:

$$P_{Hj} = U_{Hj} I_{Hj} = U_{HP} I_{Hj} \tag{4}$$

It can be seen from (4) that when the system is in steady state operation, U_{HP} is constant, and the output current I_{Hj} of each DCWT after step-up conversion is only related to its output active power. This means that the higher the output active power of a single DCWT is, the larger its output current will be; the lower the output active power of a single DCWT is, the smaller its output current will be.

According to the analysis of (2) and (4), in a parallel all-DC wind farm, each DCWT after step-up conversion is independent of each other, and the change of operation condition of a single DCWT only affects the total active power P_{HP} output by the wind farm and the current of the HVDC transmission line I_{HP}, but has no influence on the output parameters of other DCWT units in the wind farm.

Finally, the total active power P_{HP} sent by the parallel wind farm is transmitted to the grid-side MMC converter station via the HVDC busbar, and then the energy is transferred to the AC grid through the AC transformer, so as to realize the efficient steady-state operation of the parallel all-DC wind power system.

C. SELF-STARTING OF THE PARALLEL ALL-DC WIND POWER SYSTEM

When the parallel all-DC wind power system starts up, it needs to send energy back from the power grid to the wind farm. First, DC bus voltage U_{HP} is established through the grid-side MMC converter station, and then the low voltage side voltage U_L of the DCWT is established through the reverse flow of the DC/DC converter energy. The direction of energy flow during system startup is shown in Fig. 9. $P_{Hj.s}$ ($j = 1, 2\ldots, n.$) is the active power absorbed by the DCWT#j when it starts up, and $P_{grid.s}$ is the total active power returned from the grid side when the system starts up.

When the energy transmitted from the grid side is collected on the DC bus, the voltage of the high voltage side port of the DC converter is U_{Hj} ($j = 1, 2\ldots, n.$) is equal to the DC bus voltage U_{HP} established by the MMC converter. In order to realize the reverse flow of DC converter energy, this paper makes the topology capable of bidirectional energy flow by inversely parallel controllable thyristors at the diodes of the input and output ports of each phase circuit of the

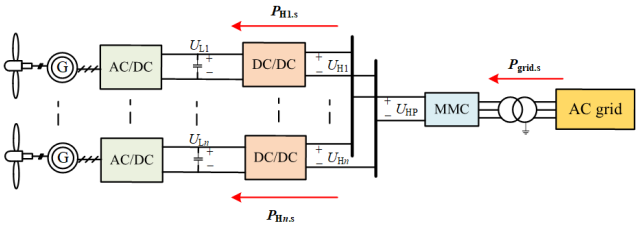

FIGURE 9. Energy flow direction of the parallel all-DC wind power system at start-up.

new DC converter. When the DCWT is started in the parallel all-DC wind power system, the energy circuit of the new DC converter is shown in Fig. 10. The isolation switches K_1 and K_2 are closed, the DC switch Q_1 is closed and Q_2 is disconnected, the switch tube T_R in the energy dissipation circuit is disconnected, and the switch device in the AC/DC converter at the machine side is locked. The electric energy flows in from the positive terminal of the high voltage DC port of the DCWT, and then flows out from the negative terminal of the high voltage DC port through the current limiting resistor R_{lim} in the charging circuit of the new DC converter, the high voltage side thyristor valve T_{HA}, n half-bridge bridge arms and n full-bridge bridge arms. At this time, n half bridge arms are connected in series with n full bridge arms, and the capacitor on the low voltage side is connected in parallel with the first half bridge arm through thyristor valve T_{LA}, realizing the establishment of the low voltage side voltage U_L in DCWT and completing the self-starting of the parallel all-DC wind power system.

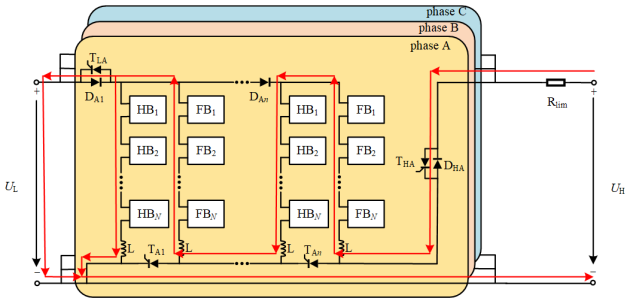

FIGURE 10. The energy flow direction of the new DC converter at start-up.

III. STEADY STATE CONTROL STRATEGY FOR THE PARALLEL ALL-DC WIND POWER SYSTEM

A. THE OVERALL CONTROL SCHEME OF THE SYSTEM

The system control block diagram of the parallel all-DC wind power system with turbine-side boost based on a new DC conversion is shown in Fig. 11. The system control block diagram mainly includes two parts: the DCWT unit based on the boost transformation and the grid-side MMC.

The generator-side AC/DC converter mainly controls the active power P_{ge} and reactive power Q_{ge} of the generator to ensure the maximum capture of wind energy [37] and the

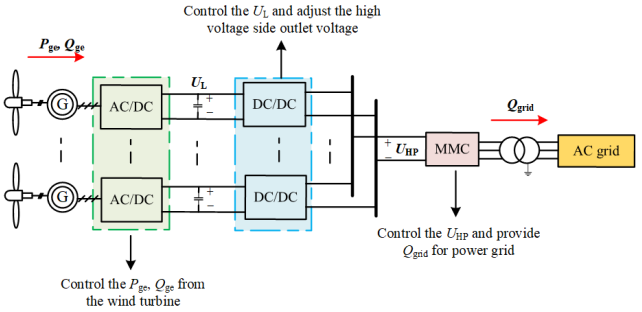

FIGURE 11. Control block diagram of the parallel all-DC wind power system.

stable operation of DCWT. The DC/DC converter is mainly used to control the stability of the low voltage side DC voltage U_L [42], and adjust the high voltage side outlet voltage of DCWT, which not only ensures the stable operation of the machine side converter, but also makes the outlet voltage of DCWT dynamically follow the change of the DC bus voltage. The grid-side MMC is mainly responsible for controlling the stability of the high voltage DC bus voltage U_{HP} and providing certain reactive power Q_{grid} support for the AC grid, so as to ensure that all the total active power output of the wind farm is transmitted to the AC grid [43].

B. CONTROL STRATEGY OF DCWT BASED ON STEP-UP CONVERSION

1) GENERATOR-SIDE AC/DC CONVERTER CONTROL STRATEGY

The generator-side AC/DC converter uses voltage source type two-level converter (VSC) and adopts d-q current vector control strategy with feedforward decoupling to control the active power P_{ge} and reactive power Q_{ge} on the machine side. The active power and reactive power output of the wind generator are controlled by real-time control of the feedback current components of axis d and q, and voltage modulation signals u_d and u_q are calculated by current feedback control, and then the voltage modulation signals are obtained by coordinate transformation to the three-phase modulation signal, and finally the control signal of the switch tube is output by PWM modulation, so as to control the steady operation of DCWT. The control strategy diagram of generator-side AC/DC converter on generator side is shown in Fig. 12.

In Fig. 12, I_a, I_b, and I_c are three-phase AC current of the converter; E_a, E_b, and E_c are three-phase AC voltage of the converter; I_d and I_q are the d and q axis components of three-phase AC current respectively; E_d and E_q are the d and q axis components of three-phase AC voltage respectively; I_{d_ref} and I_{q_ref} are the given values of d and q axis of the three-phase AC current respectively; u_d and u_q are the d and q axis components of the three-phase modulated signal respectively; u_{ga_ref}, u_{gb_ref}, and u_{gc_ref} are three-phase modulation signals; PLL is phase-locked loop controller;

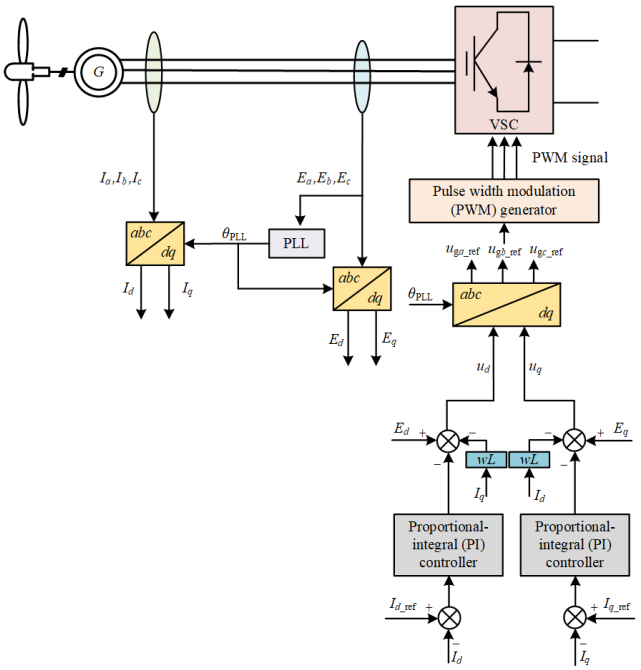

FIGURE 12. The control strategy block diagram of generator-side AC/DC converter.

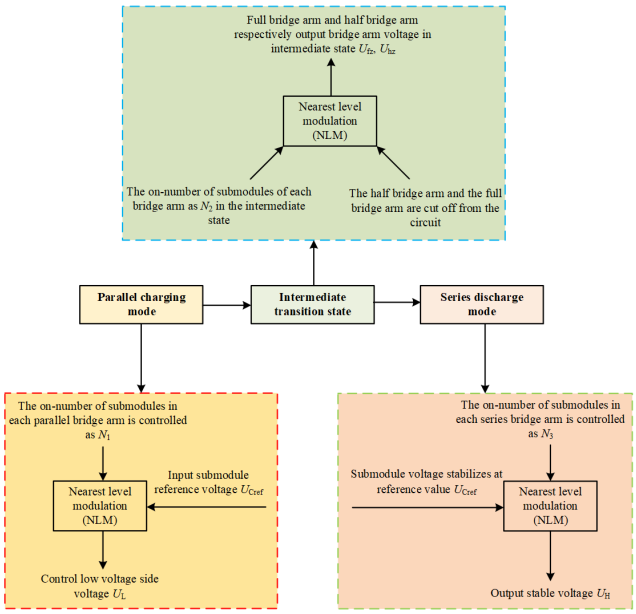

FIGURE 13. Control strategy block diagram for each phase circuit of new DC converter.

θ_{PLL} is the phase angle of A-phase voltage at AC side; wL is the reactance value of the single-phase line on the AC side.

2) NEW DC CONVERTER CONTROL STRATEGY

In the steady operation of the parallel all-DC wind power system, the new DC converter is mainly responsible for controlling the stability of the low voltage side voltage U_L in the DCWT, and regulating the outlet voltage of the high voltage side, so as to ensure the stable operation of the DCWT after the step-up conversion. The control strategy block diagram for each phase circuit of new DC converter is shown in Fig. 13.

The control strategy for each phase circuit of new DC converter is an open loop control strategy based on the nearest level modulation (NLM). Suppose there are n full bridge arms and n half bridge arms in each phase circuit, and there are N full bridge or half bridge submodules in each bridge arm. In order to ensure the continuity of the low voltage side current and high voltage side voltage, the new DC converter adopts the operation mode with a three-phase difference of 120 degrees, that is, the phase difference between the parallel charging mode or the series discharge mode between each phase circuit is 120 degrees. Under this operation mode, the parallel charging mode and series discharging mode in each phase circuit account for 120 degrees respectively. In order to make the charging and discharging modes of each phase circuit connect stably, an intermediate transition state is introduced in the control period of each phase circuit.

In the parallel charging mode, n full bridge arms are connected to n half bridge arms in parallel. By means of the nearest level modulation, the capacitor voltage of all submodules in each bridge arm reaches the reference voltage U_{Cref}, and the number of conducting submodules on each bridge arm is controlled as N_1, so that the voltage on the low voltage side reaches the given value U_{Lref}. In parallel charging mode, the relation between capacitor voltage U_c of submodules, the number of conducting submodules each bridge arm N_1, low-voltage side voltage U_L, half-bridge arm voltage U_{hb}, and full-bridge arm voltage U_{fb} can be expressed as:

$$N_1 U_c = U_L = U_{hb} = U_{fb} \tag{5}$$

In the intermediate transition state, n full bridge arms and n half bridge arms are disconnected from the circuit, and the number of conducting submodules on each bridge arm is controlled as N_2, so that the half-bridge arms and full bridge arms output the intermediate state voltage U_{hz} and U_{fz} respectively. In the intermediate transition state, the relationship between the capacitor voltage U_c of submodules, the number of conducting submodules each bridge arm N_2, the voltage of half-bridge arm U_{hz}, and the voltage of full-bridge arm U_{fz} can be expressed as:

$$N_2 U_c = U_{hz} = U_{fz} \tag{6}$$

In series discharge mode, n full bridge arms are connected in series with n half bridge arms, and the number of conducting submodules on each bridge is controlled to be N_3, so that the sum of capacitor voltage of all conducting submodules in series follows the DC bus voltage U_{HP}. At this time, the relationship between the outlet voltage U_H of DCWT, DC bus voltage U_{HP}, capacitor voltage U_c of submodules, the number of conducting submodules each bridge arm N_3, half-bridge arm voltage U_{hc}, and full-bridge arm voltage U_{fc} can be

expressed as:

$$\begin{cases} nU_{\mathrm{hc}} + nU_{\mathrm{fc}} = U_{\mathrm{H}} \\ N_3 U_{\mathrm{c}} = U_{\mathrm{hc}} = U_{\mathrm{fc}} \\ U_{\mathrm{H}} = U_{\mathrm{HP}} \end{cases} \tag{7}$$

C. CONTROL STRATEGY OF THE GRID-SIDE MMC

When the system runs in a steady state, the grid-side MMC converter mainly controls the voltage of the high voltage DC bus U_{HP}, so that all the active power output from the wind farm is transferred to the AC grid, and provides a certain reactive power Q_{grid} for the AC grid to ensure the stable operation of the AC grid [44].

The grid-side MMC converter adopts double closed-loop control strategy [45], including voltage outer loop and current inner loop control, with fast current response characteristics and good internal current limiting ability. In this strategy, the outer loop mainly generates the d-axis reference current instruction I_{d1_ref} by controlling the DC bus voltage U_{HP} to reach the given value, and controls the reactive power Q_{grid} to generate the q-axis reference current instruction I_{q1_ref}. Then the three phase voltage modulation signal is obtained by the inner loop current control. The control strategy block diagram is shown in Fig. 14, where U_{HPref} is the given value of DC bus voltage; U_{HP} is the voltage feedback value of DC bus; $Q_{\mathrm{grid\_ref}}$ is the given value of reactive power transmitted to the grid side; U_d is the amplitude of AC phase voltage at the grid side; I_{d1_ref} and I_{q1_ref} are the given values of d axis and q axis of the three-phase current at the grid side respectively; I_{d1} and I_{q1} are respectively the feedback values of d and q axis components of three-phase AC current at the grid side; E_{d1} and E_{q1} are the d and q axis components of three-phase AC voltage at the grid side respectively; u_{d1} and u_{q1} are respectively the d and q axis components of the three-phase voltage modulated signal; u_{a_ref}, u_{b_ref}, and u_{c_ref} are three-phase modulation signals; wL_1 is the reactance value of the single-phase AC line on the grid side.

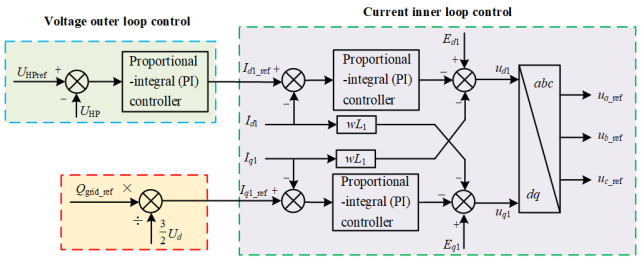

FIGURE 14. Control strategy block diagram of the grid-side MMC.

IV. FAULT HANDLING STRATEGY OF THE PARALLEL ALL-DC WIND POWER SYSTEM

A. FAILURE OF DCWT

When a DCWT in the parallel all-DC wind power system fails due to internal mechanical components, transmission lines or control systems, the DCWT needs to be taken out of operation and repaired to avoid influence on the stable operation of the system. The switching logic of the faulty DC wind turbine is shown in Fig. 15.

In this paper, a bypass switch is added at the high voltage outlet of the DCWT based on the boost voltage transformation, so that the faulty DCWT unit can be stably removed, so as to improve the reliability of the system operation.

As can be seen from Fig. 15, when a DCWT fails, the switching logic of the faulty turbine mainly includes the following steps:

Step 1: by disconnecting isolation switches K_1 and K_2 and closing DC switches Q_1 and Q_2 in the charging circuit, the DC wind turbine is cut off.

Step 2: by locking the switching device in AC/DC converter, cutting out the submodules in the new DC converter, and closing the switching tube T_R in the energy dissipation circuit, the electric energy in the DC wind turbine is released through the energy dissipation circuit.

Step 3: If the faulty DCWT can be started by reset, T_R and Q_2 will be disconnected, K_1, K_2, and Q_1 will be closed, and DCWT will resume to start.

Step 4: If it cannot be started by reset, the DC wind turbine needs to be repaired. After the maintenance of the faulty DCWT is completed, the DCWT can be restarted by disconnecting T_R and Q_2, and closing K_1, K_2, and Q_1.

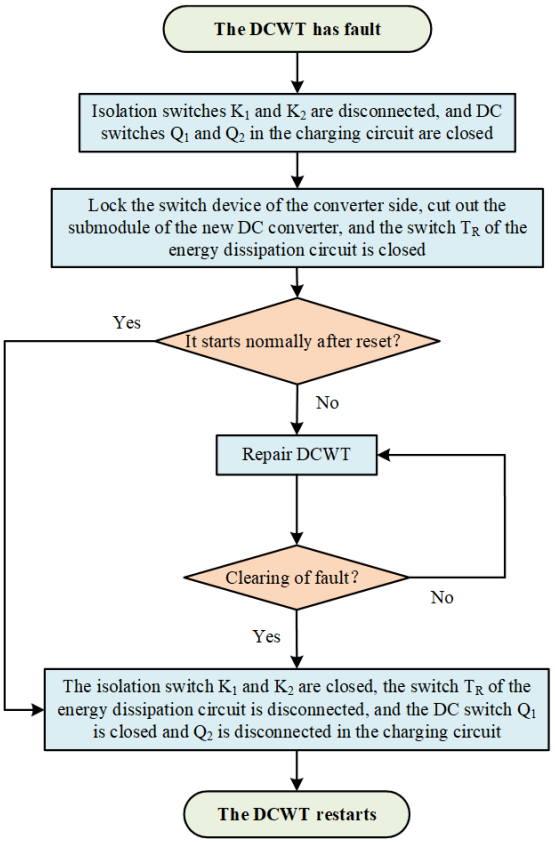

FIGURE 15. The switching logic of the faulty DCWT.

B. DC BUS SHORT CIRCUIT FAULT

When the HVDC line short circuit fault occurs in the parallel all-DC wind power system, the voltage at the fault point will drop rapidly and the current will rise rapidly, which will seriously harm the safe operation of each part of the converter devices in the system [46], [47]. Therefore, the DCWT and the grid-side MMC must be able to clear the short-circuit fault current at the DC side to ensure that the switch components in the system are not burned during the fault.

1) DC BUS SHORT CIRCUIT FAULT HANDLING OF DCWT

a short circuit fault occurs in the high voltage DC side of the DCWT based on the step-up conversion, the submodules of all the bridge arms in the new DC converter in the DCWT are locked. The flow path of fault current in DCWT is shown in Fig. 16.

In Fig. 16, $U_{\mathrm{c.H}i}$ ($i = 1, 2\ldots, N.$) are the capacitance voltage of the submodules of the half-bridge arm; $U_{\mathrm{c.F}i}$ ($i = 1, 2\ldots, N.$) are the capacitance voltage of the submodules of the full-bridge arm; U_{Fq} is the full-bridge arm voltage and U_{Hq} is the half-bridge arm voltage.

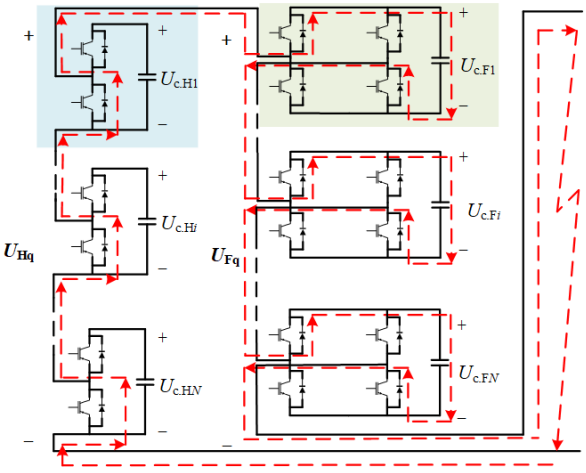

FIGURE 16. The flow path of fault current in DCWT.

As can be seen from Fig. 16, the short circuit current only flows in series mode of the new DC converter and only passes through the capacitance of the full bridge arm submodule. In addition, the direction of short circuit current is the same as the direction of capacitor voltage of the full bridge submodule, which is the direction of capacitor charging of the full bridge submodule. As a result, the full bridge arm outputs positive voltage along the direction of short circuit current, whereas the output voltage of the half bridge arm is zero, so as to drive the fault current to rapidly decay to zero. Half-bridge arm voltage U_{Hq} and full-bridge arm voltage U_{Fq} can be expressed as:

$$\begin{cases} U_{\mathrm{Hq}} = 0 \\ U_{\mathrm{Fq}} = \sum_{i=1}^{N} U_{\mathrm{c.F}i} \end{cases} \tag{8}$$

In addition, since the output power of the high voltage side of the DCWT drops to zero during the short circuit fault of the DC bus, in order to consume the active power emitted by the DCWT during the fault period and prevent the voltage of the low voltage side from increasing due to power surplus, the switch tube T_R in the energy dissipation circuit should be closed during the fault period, and the energy dissipation resistor R_C should be put in to consume the power emitted by the wind generator.

If the DC bus short-circuit fault is cleared within the allowable failure time of the wind turbine, it is necessary to unlock the DC/DC switching device in the DCWT and disconnect the T_R in the energy dissipation circuit, so that the DCWT can restore normal operation. If the DC bus short-circuit fault cannot be cleared within a short time, the fault is considered as a permanent fault, and all wind turbines in the wind farm must be shut down.

2) DC BUS SHORT CIRCUIT FAULT HANDLING OF THE GRID-SIDE MMC

In order to suppress the fault current when the DC bus is short circuit, the grid-side MMC adopts the hybrid topology of full bridge and half bridge submodules [48], [49]. The flow path of the fault current in the MMC at the grid side is shown in Fig. 17.

In Fig. 17, $U_{\mathrm{c.aF1}}$, $U_{\mathrm{c.aF2}}$, $U_{\mathrm{c.bF1}}$, $U_{\mathrm{c.bF2}}$, $U_{\mathrm{c.cF1}}$, and $U_{\mathrm{c.cF2}}$ are the capacitance voltage of the full bridge submodule in the three-phase bridge arm respectively; U_{apn} is the A-phase bridge arm voltage. During the fault period, the switching device of the grid-side MMC is locked, and the short circuit current only passes through the capacitor of the full bridge submodule, whose direction is the same as that of the capacitor charging of the full bridge submodule, so that the output voltage of the MMC bridge arm is opposite to the direction of the short-circuit current, forming negative pressure and providing back electromotive force to suppress the fault current. Taking the A-phase bridge arm voltage as an example, it can be expressed as:

$$U_{\mathrm{apn}} = -(U_{\mathrm{c.aF1}} + U_{\mathrm{c.aF2}}) \tag{9}$$

If the DC bus short-circuit fault is cleared within the allowable failure time of the wind turbine, it is necessary to unlock the MMC switch on the grid side, so that the output power of the wind farm can be normally transmitted to the grid. If the DC bus short-circuit fault cannot be cleared within a short time, the fault is considered as a permanent fault, and the converter station needs to stop.

V. OPERATION ANALYSIS OF THE PROPOSED WIND POWER SYSTEM TOPOLOGY

In terms of operational flexibility and safety reliability, a series wind farm topology is proposed in [42] and [50] by respectively using DC/DC converters based on H-bridge structure and single-phase hybrid modular multilevel converter type DC transformers. However, due to the series of wind turbines, the coupling effect between wind turbines

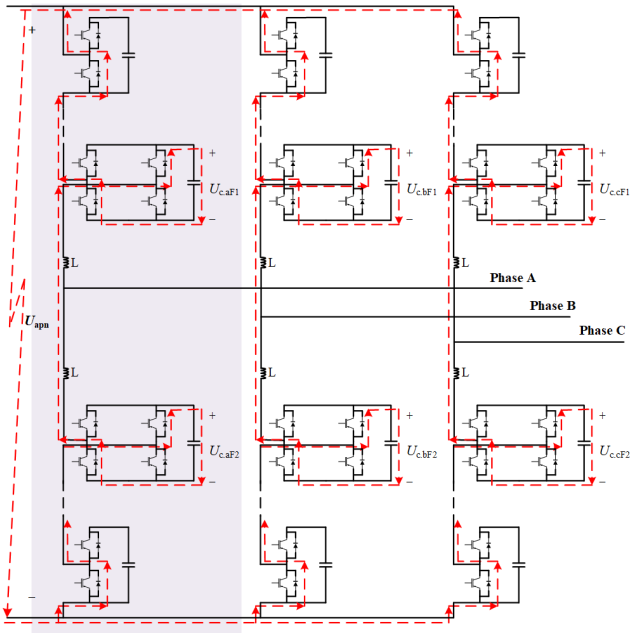

FIGURE 17. The flow path of fault current in grid-side MMC.

is increased, which greatly improves the control difficulty of the system and limits the control flexibility of its topology. In order to solve the overvoltage problem, a topology structure of wind power system based on modular multiphase PMSG is proposed in [51]. However, the designed power-voltage coordinated control strategy of wind farm is complicated, and the safety and reliability of its topology need to be further studied. Compared with the above research, the proposed parallel all-DC wind farm topology based on the new DC converter avoids the problems of coupling and outlet overvoltage of the wind turbine in the above topology, and greatly improves the control flexibility and safety reliability of the wind farm.

In terms of self-starting mode, compared with the wind farm topology based on DAB modular DCSST topology adopted in the current [40], the DC wind farm topology based on the new DC converter adopted in this paper can realize the energy return from the high voltage side and low voltage side of each phase circuit by controlling the bridge arms in series with each other in each phase circuit, and conducting the anti-parallel thyristors on the low and high voltage sides, which not only avoids the circulation problem caused by the imbalance of DAB power distribution [41] during the self-start of the wind farm based on DAB modular DCSST, but also reduces the difficulty of the self-start control of the wind farm. In addition, compared with the self-starting method of wind farm based on energy storage charging adopted in [52], this paper reduces additional equipment investment and the difficulty of coordinated control of various converters during operation of wind farm through the advantages of topology itself.

In terms of dealing with DC short circuit faults, the wind farm topologies based on DAB modular DCSST topology [40] and the wind farm topologies using dual phase-shifted three-level DC/DC converters [53], [54] are often connected with additional inductors and switching circuits [55] at the outlet of the DC converter in order to clear DC short circuit faults. By blocking the secondary capacitor discharge circuit and increasing the secondary inductance during the DC short-circuit fault, the topology can realize fault crossing without locking. However, due to the use of additional switching devices and inductors in the above DC short circuit fault handing method, not only increases the investment in circuit design and the loss of switching devices during steady-state operation of the circuit, but also increases the breaking voltage stress of the active switch tube at the wind turbine outlet, and reduces the reliability of dealing with DC short circuit faults. The topological structure of the wind farm based on the new DC converter proposed in this paper does not need additional auxiliary circuit to isolate the DC fault, and only needs to lock the switching tube of the new DC converter to cut off the fault current. Compared with the above approach, the topology proposed in this paper not only reduces the extra investment and operating loss, but also greatly improves the reliability during the DC short-circuit fault ride-through period. Compared with the method of using energy storage to solve DC short circuit fault [56], the topology proposed in this paper reduces the additional equipment investment of the system according to its own advantages and avoids complex fault control operations.

VI. SIMULATION STUDY

In order to verify the feasibility and effectiveness of the proposed parallel all-DC wind power system topology scheme and its control strategy, a simulation model of the parallel all-DC wind power system with turbine-side boost based on a new DC conversion of 10WM was built based on PSCAD/EMTDC, as shown in Fig. 18. In the system, the generator-side AC/DC converter of DCWT adopts a two-level voltage source converter, the DC/DC converter adopts a new DC converter with parallel charging and series discharge, and the grid-side DC/AC converter at the grid side adopts a modular multilevel converter.

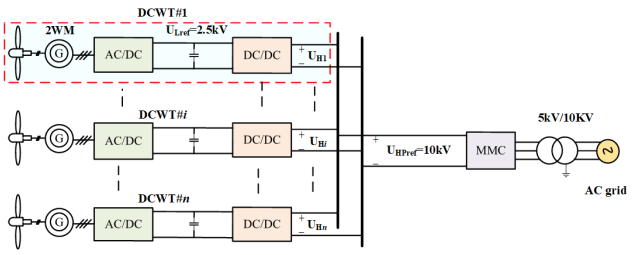

FIGURE 18. Simulation model of the parallel all-DC wind power system.

The main parameters of the system in Fig. 18 are shown in Table 1, where P_{HPref} is the rated capacity of the wind

TABLE 1. Main simulation parameters of the system.

Parameter	Value
P_{HPref} (MW)	10
n	5
P_{Href} (MW)	2
f_{v} (Hz)	2000
U_{Cref} (kV)	1.25
U_{Lref} (kV)	2.5
U_{HPref} (kV)	10
f_{m} (Hz)	500
U_{s} (kV)	5

farm; n is the number of DCWT in the wind farm; P_{Href} is rated capacity of the DCWT; f_{v} is the switching frequency of AC/DC converter on the machine side; U_{Cref} is the rated voltage of the new DC converter submodule; U_{Lref} is the reference value of DC voltage on the low voltage side of the new DC converter; U_{HPref} is the reference value of DC bus voltage; f_{m} is the switching frequency of MMC at the grid side; U_{s} is the effective value of the AC line voltage at the grid side.

A. THE DCWT RUNS IN STEADY STATE

Fig. 19 shows the system simulation waveform when all DCWT units in the wind farm are running stably at rated working conditions.

As can be seen from the simulation results in Fig. 19, when all DCWT units operate stably at rated operating conditions, the low-voltage side voltage, high-voltage side output voltage, output current, and output active power of all DCWT units are stabilized at 2.5kV, 10kV, 0.2kA, and 2WM respectively, and the relationship between output current and output active power of each DCWT satisfies (4). The collecting current of the DC bus is 1kA, and the relation between it and the output current of each DCWT satisfies (3). The total output active power of the wind farm is 10MW, and the relation between it and the output active power of each DCWT satisfies (2).

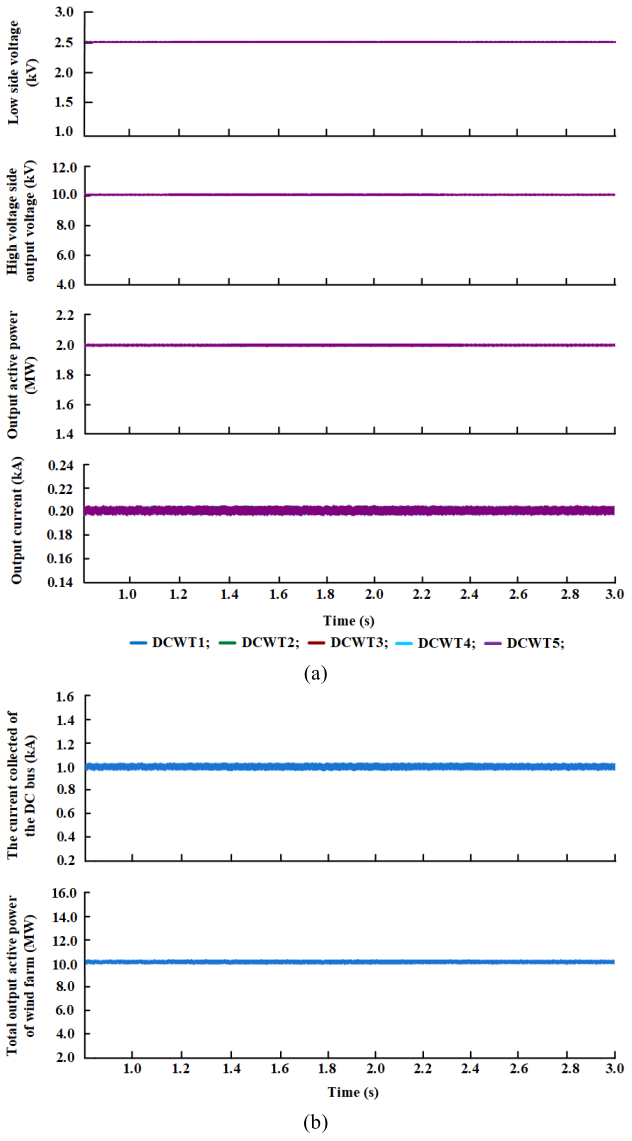

FIGURE 19. System waveform when all DCWT units are stable under rated operating conditions.

B. THE DCWT RUNS DYNAMICALLY

Fig. 20 shows the system waveform when the active power output of two DCWT units (No. 1 and No. 2) in the wind farm changes dynamically. The output power of DCWT#1 and DCWT#2 changed from 2.0MW to 1.2MW at 1.5s, and from 1.2MW to 1.6MW at 2.5s.

By observing the simulation results in Fig. 20, it can be concluded that:

1) When the active power output of DCWT changes, the DC voltage on the low voltage side and high voltage side of the DC/DC converter of DCWT does not change, and the voltage on both sides can be stable at the rated value.

2) The output current of the high voltage side of the DCWT in dynamic operation changes with the change of the output active power, and finally reaches a new equilibrium after a short period of fluctuation, which conforms to the dynamic operation characteristics of the parallel all-DC wind farm.

3) Changes in the active power output of a single DCWT unit in the parallel all-DC wind farm will not affect other DCWT units rated for operation, which proves that the operation of each DCWT has independent controllability. When a DCWT is in dynamic operation, the collecting current of the DC bus and the active power output of the wind farm change correspondingly, which conforms to the output characteristics of the wind farm.

Therefore, it can be concluded from the above analysis that this topology scheme can not only maintain the safe and stable operation of the wind power system, but also send out all the active power output of all DCWT units when the active

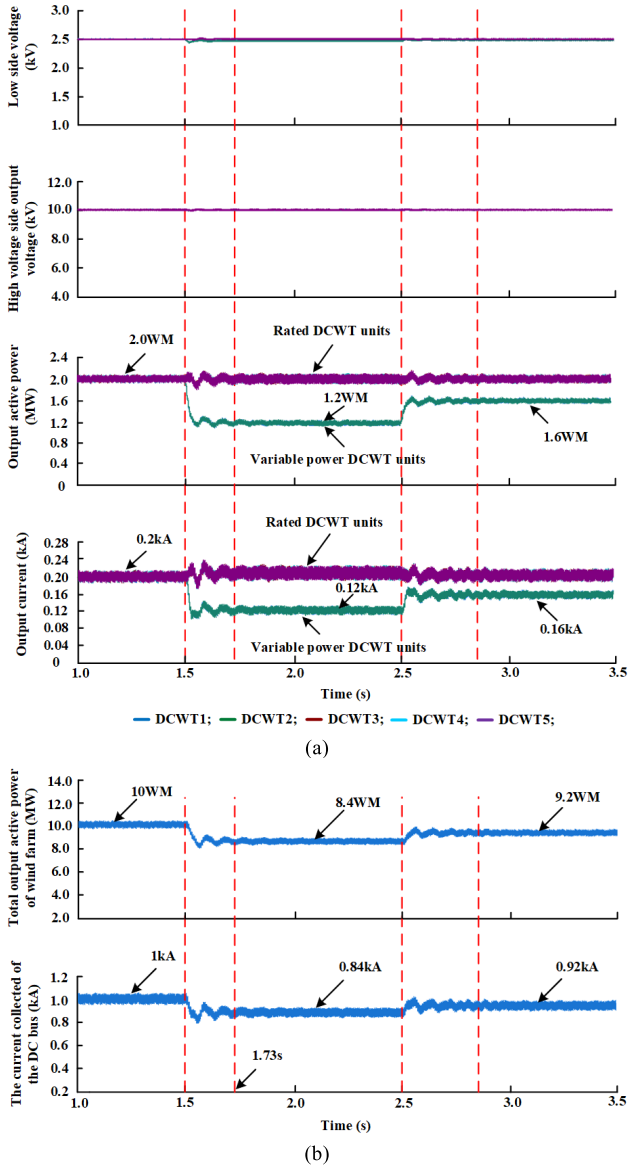

FIGURE 20. System waveform when DCWT is running dynamically.

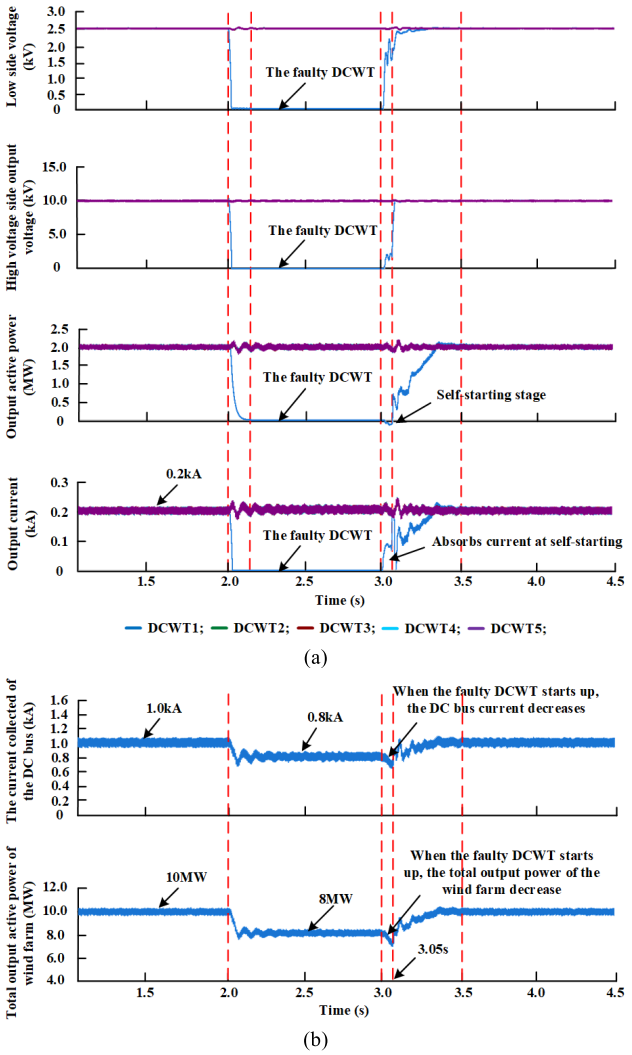

FIGURE 21. System waveform when the DCWT1 is faulty.

power output of multiple DCWT units changes due to wind speed or control reasons.

C. THE FAULTY DCWT CUTS OUT AND IN

Simulation waveform of the parallel all-DC wind power generation system when DCWT#1 fails is shown in Fig. 21. Before 2s, all DCWT units in the all-DC wind farm operate at rated state. At 2s, DCWT#1 is removed due to a fault. At 3s, the DCWT#1 will be redeployed through self-starting after being repaired.

By observing the simulation results in Fig. 21, it can be concluded that:

1) Before 2s, all DCWT units run at rated state, and the voltage of the low voltage side, the output voltage of the high voltage side, the output active power, and the output current of the high voltage side are stabilized at 2.5kV, 10kV, 2MW and 0.2kA respectively. The total active power delivered by the wind farm to the grid side is 10MW, and the collecting current of the DC bus is 1kA.

2) DCWT#1 fails at 2s. Firstly, the DCWT#1 is disconnected by isolating switches K_1 and K_2. Then the switching devices in the rectifier are blocked, and the submodules in the new DC converter are cut out. Finally, the internal power of the DCWT is released by closing the switch tube T_R in the energy dissipation circuit. At this time, the DC voltage on the low voltage side of the new DC converter drops to zero because of the capacitor discharge. In addition, because all the submodules in the new DC converter are cut out, the output voltage and current of the DCWT are reduced to zero, making the output active power of the DCWT drop to zero. Moreover, because DCWT#1 was cut out due to failure, the total active power delivered by the DC wind farm to the grid side decreased to 8MW, resulting in the collecting current of the DC bus decreased to 0.8kA after a short fluctuation. The

output active power and low-voltage side voltage of other DCWT units in normal operation are restored to the rated value after a brief fluctuation.

3) DCWT#1 will be put back into operation after maintenance at 3s. Firstly, the isolation switch K_1 and K_2 are closed and the switch tube T_R in the energy dissipation circuit is disconnected. Then, by turning the DC switch Q_1 on and Q_2 off, the charging resistor R_{lim} is put in. Finally, by re-putting the submodule in the new DC converter, the DC support capacitor on the low voltage side builds voltage, so that DCWT#1 can absorb active power to realize self-starting. Restore DCWT#1 to normal operation at 3.05s by unlocking the switch tube of AC/DC converter. During the self-starting of DCWT#1, part of the total active power output of other 4 DCWT units in normal operation is transmitted to DCWT#1 for self-starting, and the remaining active power is transmitted to the grid side. At this time, the active power output of and RMS current output of DCWT in the wind farm can be expressed as:

$$\sum_{j=2}^{5} P_{Hj} = P_{HP} - P_{H1} + P_{Rl} \tag{10}$$

$$\sum_{j=2}^{5} I_{Hj} = I_{H1} + I_{HP} \tag{11}$$

In (10), $-P_{H1}$ is the active power absorbed by DCWT#1 during its self-starting; P_{Rl} is the active power consumed by charging resistance R_{lim} when DCWT#1 starts up. P_{HP} is the total active power transmitted by the wind farm to the grid side.

In (11), I_{H1} is the effective value of output current during the startup of DCWT#1; I_{HP} is the effective value of the collecting current of the DC bus.

From the above analysis, it can be seen that when a DCWT in the all-DC wind farm fails, the whole wind farm can quickly adjust the output and maintain the stable operation of the wind farm. During the self-starting period of the faulty DCWT, the faulty DCWT can successfully realize self-starting by absorbing part of the active power output of other DCWT units in normal operation, which not only ensures the stable operation of other DCWT units, but also realizes the safe transmission of active power output of wind farm.

D. DC BUS SHORT CIRCUIT FAULT

When DC busbar short-circuit fault occurs, the grid-side MMC can realize the rapid removal of short circuit current through the locking submodule, and the wind farm can realize the rapid removal of short circuit current at the turbine-side and the reasonable consumption of surplus power through the internal processing of all DCWT units. When DC bus short-circuit fault occurs, the simulation waveform of output parameter of all DCWT units is shown in Fig. 22.

By observing the simulation results in Fig. 22, it can be concluded that:

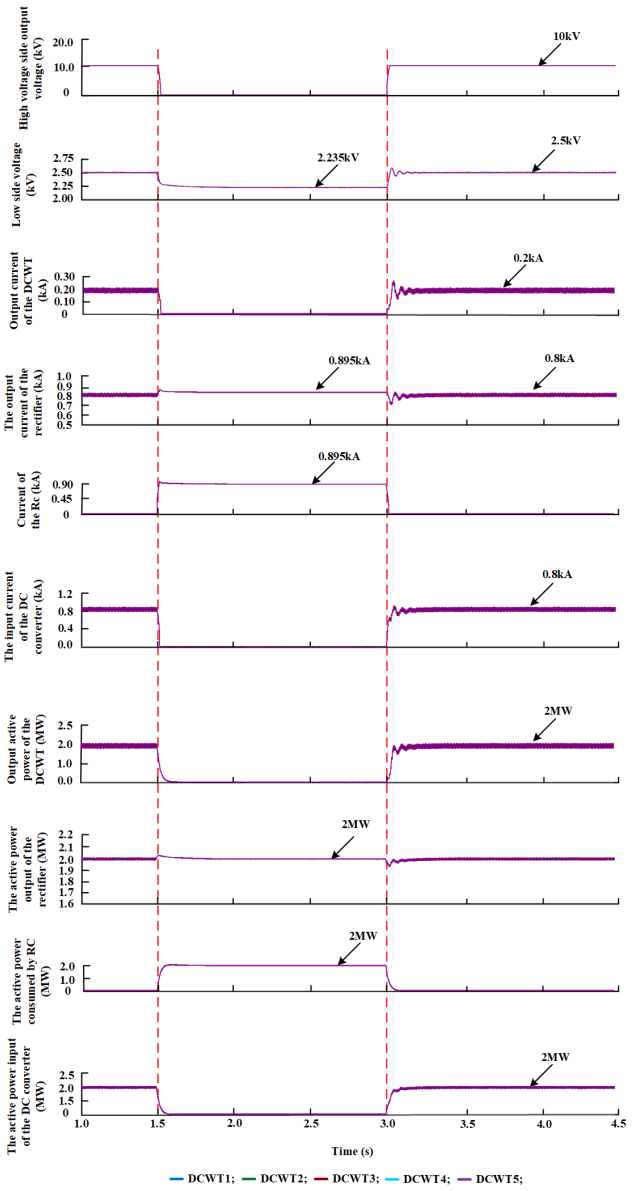

FIGURE 22. Output parameter waveform of all DCWT units in case of DC bus short circuit fault.

1) Before 1.5s, all DCWT units run at rated state with output active power of 2MW, voltage of low voltage side of 2.5kV, output voltage of high voltage side of 10kV, and output current of 0.2kA.

2) During the period from 1.5s to 3.0s, DC bus has short circuit fault. The switching devices of the new DC converter in all DCWT units are closed, and the all resistances R_C input in the energy dissipation circuit. At this time, the output voltage, the outlet circuit current, and the output active power of all DCWT units quickly become zero. As the output active power of all DCWT units become zero, the input current and input power of all new DC converters both drop to zero. The all resistances R_C of the energy dissipation circuit consume the active power emitted by the wind generator, and the

current, voltage, and active power consumed on the each R_C reach a stable value of 0.895kA, 2.235kV, and 2MW respectively after a short fluctuation. This indicates that the above measures can not only quickly cut off the short circuit current during the short circuit of the DC bus, but also eliminate the influence of the rise of low voltage side voltage in all DCWT units due to power surplus.

3) At 3.5s, DC bus short circuit fault is cleared. At this time, by unlocking the switching devices of the grid-side MMC and the new DC converters of all DCWT units in the wind farm, and removing all resistances R_C in the energy dissipation circuit, the parallel all-DC wind power generation system resume normal operation.

VII. CONCLUSION

In order to improve the control flexibility of all-DC wind farms, reduce the difficulty of self-starting control, and ensure the high reliability of DC fault crossing, this paper first proposed a topological structure of all DC wind power system based on a novel DC transform. Then, the operation characteristics of the parallel wind farm were analyzed, and the control strategies under different operating conditions were designed. Finally, the feasibility of the topology and the effectiveness of the control strategy were verified by simulation. The theoretical analysis and simulation results show that:

1) The parallel all-DC wind farm with turbine-side boost based on a new DC conversion can effectively realize flexible control during steady and dynamic operation of the wind farm on the premise of ensuring the stable operation of each conversion device in the wind farm.

2) By controlling the connection mode of each bridge arm of the new DC converter, the wind farm can realize self-starting under low control difficulty.

3) When a DC short-circuit fault occurs at the DC bus bar, by blocking the switching device of the new DC converter, the parallel all-DC wind farm with turbine-side boost based on a new DC conversion not only realizes the rapid removal of DC fault current, effectively guarantees the safety of the all-DC wind farm during the DC fault period, but also enables the wind farm to resume normal operation after the fault removal, greatly improving the reliability of the wind farm in the DC fault crossing.

REFERENCES

[1] S. Rodrigues, C. Restrepo, E. Kontos, R. T. Pinto, and P. Bauer, "Trends of offshore wind projects," *Renew. Sustain. Energy Rev.*, vol. 49, pp. 1114–1135, Sep. 2015.

[2] J. L. Rodríguez-Amenedo, S. Arnaltes-Gómez, M. Aragüés-Peñalba, and O. Gomis-Bellmunt, "Control of the parallel operation of VSC-HVDC links connected to an offshore wind farm," *IEEE Trans. Power Del.*, vol. 34, no. 1, pp. 32–41, Feb. 2019.

[3] G. Yang, "Review on engineering practices and future technology prospects of European offshore wind power," *Automat. Electr. Power Syst.*, vol. 45, no. 21, pp. 23–32, 2021.

[4] M. H. J. Bollen and K. Yang, "Harmonic aspects of wind power integration," *J. Modern Power Syst. Clean Energy*, vol. 1, no. 1, pp. 14–21, Jun. 2013.

[5] D. Patel, R. K. Varma, R. Seethapathy, and M. Dang, "Impact of wind turbine generators on network resonance and harmonic distortion," in *Proc. CCECE*, Calgary, AB, Canada, May 2010, pp. 1–6.

[6] Z. Xu, Y. Jin, S. Li, and Z. Zhang, "Mechanism analysis and mitigation of harmonic resonance amplification caused by AC integration of offshore wind farm," *Automat. Electr. Power Syst.*, vol. 45, no. 21, pp. 85–91, 2021.

[7] D. Zhao, J. Ma, M. Qian, L. Zhu, H. Han, and Y. Liu, "Reactive power configuration and coordinated control of offshore wind farms connected to power grid with AC cables," *Power Syst. Technol.*, vol. 41, no. 5, pp. 1412–1418, 2017.

[8] X. Li, A. Gayan, L. Yao, J. Liang, and F. Cheng, "Recent development and prospect of offshore wind power in Europe," *J. Global Energy Interconnection*, vol. 2, no. 2, pp. 116–126, 2019.

[9] X. Cai, G. Shi, Y. Chi, Y. Chang, R. Yang, and Z. Zhang, "Present status and future development of offshore all-DC wind farm," *Proc. CSEE*, vol. 36, no. 8, pp. 2036–2048, 2016.

[10] Z. Chen, J. M. Guerrero, and F. Blaabjerg, "A review of the state of the art of power electronics for wind turbines," *IEEE Trans. Power Electron.*, vol. 24, no. 8, pp. 1859–1875, Aug. 2009.

[11] N. Holtsmark, H. J. Bahirat, M. Molinas, B. A. Mork, and H. K. Hoidalen, "An all-DC offshore wind farm with series-connected turbines: An alternative to the classical parallel AC model?" *IEEE Trans. Ind. Electron.*, vol. 60, no. 6, pp. 2420–2428, Jun. 2013.

[12] E. Veilleux and P. W. Lehn, "Interconnection of direct-drive wind turbines using a series-connected DC grid," *IEEE Trans. Sustain. Energy*, vol. 5, no. 1, pp. 139–147, Jan. 2014.

[13] F. Deng and Z. Chen, "Operation and control of a DC-grid offshore wind farm under DC transmission system faults," *IEEE Trans. Power Del.*, vol. 28, no. 3, pp. 1356–1363, Jul. 2013.

[14] C. Zhan, C. Smith, A. Crane, A. Bullock, and D. Grieve, "DC transmission and distribution system for a large offshore wind farm," in *Proc. 9th IET Int. Conf. AC DC Power Transmiss. (ACDC)*, Oct. 2010, pp. 1–5.

[15] F. Rong, G. Wu, X. Li, S. Huang, and B. Zhou, "ALL-DC offshore wind farm with series-connected wind turbines to overcome unequal wind speeds," *IEEE Trans. Power Electron.*, vol. 34, no. 2, pp. 1370–1381, Feb. 2019.

[16] L. Yao, G. Shi, Y. Cao, Z. Wang, M. Zhu, and X. Cai, "Variable speed control of series-connected DC wind turbines in the internal grid of offshore DC wind farm," *Power Syst. Technol.*, vol. 38, no. 9, pp. 2410–2415, 2014.

[17] S. Chuangpishit, A. Tabesh, Z. Moradi-Shahrbabak, and M. Saeedifard, "Topology design for collector systems of offshore wind farms with pure DC power systems," *IEEE Trans. Ind. Electron.*, vol. 61, no. 1, pp. 320–328, Jan. 2014.

[18] B. Zhao, F. An, L. Qu, Z. Yu, Q. Song, and R. Zeng, "Multi-function DC-collector concept and its all-DC offshore wind power system," *Proc. CSEE*, vol. 41, no. 18, pp. 6169–6180, 2021.

[19] C. Wang and J. Guo, "Research on topological structures for DC grid-connection of wind farm," *Power Syst. Technol.*, vol. 38, no. 11, pp. 3065–3070, 2014.

[20] C. Meyer, M. Hoing, A. Peterson, and R. De Doncker, "Control and design of DC-grids for offshore wind farms," in *Proc. Conf. Rec. IEEE Ind. Appl. Conf., 41st IAS Annu. Meeting*, Oct. 2006, pp. 1148–1154.

[21] Q. Liu, S. Fan, C. Hong, X. Guo, H. Tang, and X. Shen, "DC/DC converter for offshore wind power transmission using composite modular structure," *Automat. Electr. Power Syst.*, vol. 46, no. 24, pp. 142–151, 2022.

[22] D. Jiang, H. Gu, R. Yin, K. Chen, Y. Liang, and Y. Wang, "Research status and developing prospect of offshore wind farm with pure DC systems," *Power Syst. Technol.*, vol. 39, no. 9, pp. 2424–2431, 2015.

[23] D. Jovcic, "Offshore wind farm with a series multiterminal CSI HVDC," *Electric Power Syst. Res.*, vol. 78, no. 4, pp. 747–755, Apr. 2008.

[24] X. Wei, X. Wang, C. Gao, and S. Zhang, "Topologies research of high voltage and high power DC/DC converters used in DC grids," *Proc. CSEE*, vol. 34, no. 1, pp. 218–224, 2014.

[25] L. Li, B. Li, J. Liu, M. Yang, D. Xu, T. Wei, and W. Li, "Ride-through strategy under commutation failure of high-voltage DC/DC transformer for all DC offshore wind farms," *Power Syst. Technol.*, vol. 46, no. 4, pp. 1391–1399, 2022.

[26] K. Shen, B. Xie, and X. Cai, "Design and simulation of modular permanent magnet DC turbine for offshore wind farm," *Electr. Mach. Control*, vol. 23, no. 2, pp. 35–43, 2019.

[27] L. Guo, G. Zhou, and L. Zhou, "Research review on high step-up ratio DC/DC converter for offshore DC wind farm," *Power Syst. Protection Control*, vol. 46, no. 12, pp. 158–169, 2018.

[28] X. Yang, T. Q. Zheng, Z. Lin, Y. Xue, Z. Wang, L. Yao, and B. Chen, "Survey of high-power DC/DC converter for HVDC grid application," *Power Syst. Technol.*, vol. 40, no. 3, pp. 670–677, 2016.
[29] K. Sano and M. Takasaki, "A boost conversion system consisting of multiple DC–DC converter modules for interfacing wind farms and HVDC transmission," in *Proc. IEEE Energy Convers. Congr. Expo.*, Denver, CO, USA, Sep. 2013, pp. 2613–2618.
[30] M. Jafari, F. Jafarishiadeh, S. Saadatmand, A. Ghasemi, A. Shojaeighadikolaei, and R. Ahmadi, "Current stress reduction investigation of isolated MMC-based DC–DC converters," in *Proc. IEEE Power Energy Conf. at Illinois (PECI)*, Champaign, IL, USA, Feb. 2020, pp. 1–4.
[31] L. Yao, X. Yang, Z. Lin, Y. Xue, X. Huang, T. Q. Zheng, Z. Wang, and Y. Li, "DC fault characteristics of modular multilevel converter based HVDC transformer," *Power Syst. Technol.*, vol. 40, no. 4, pp. 1051–1058, 2016.
[32] S. Kenzelmann, A. Rufer, M. Vasiladiotis, D. Dujic, F. Canales, and Y. R. de Novaes, "A versatile DC–DC converter for energy collection and distribution using the modular multilevel converter," in *Proc. 14th Eur. Conf. Power Electron. Appl.*, Birmingham, U.K., Aug. 2011, pp. 1–10.
[33] W. Lin, "DC–DC autotransformer with bidirectional DC fault isolating capability," *IEEE Trans. Power Electron.*, vol. 31, no. 8, pp. 5400–5410, Aug. 2016.
[34] B. Li, X. Zhao, D. Cheng, S. Zhang, and D. Xu, "Novel hybrid DC/DC converter topology for HVDC interconnections," *IEEE Trans. Power Electron.*, vol. 34, no. 6, pp. 5131–5146, Jun. 2019.
[35] B. Li, J. Liu, Z. Wang, S. Zhang, and D. Xu, "Modular high-power DC–DC converter for MVDC renewable energy collection systems," *IEEE Trans. Ind. Electron.*, vol. 68, no. 7, pp. 5875–5886, Jul. 2021.
[36] R. Yin, D. Jiang, W. Tang, Y. Zhou, Y. Liang, and Y. Du, "Modular isolated DC/DC converter based grid-connection scheme for offshore DC wind farm," *Automat. Electr. Power Syst.*, vol. 40, no. 17, pp. 190–196, 2016.
[37] X. Wang, G. Tang, Z. He, X. Wei, C. Ma, S. Zhang, and X. Xiao, "Topology research of DC/DC converters for offshore wind farm DC collection systems," *Proc. CSEE*, vol. 37, no. 3, pp. 837–847, 2017.
[38] S. M. Muyeen, A. Al-Durra, and J. Tamura, "Transmission of bulk power from DC-based offshore wind farm to grid through HVDC system," *Green Energy Technol.*, vol. 78, pp. 501–520, 2012.
[39] F. Deng and Z. Chen, "An offshore wind farm with DC grid connection and its performance under power system transients," in *Proc. IEEE Power Energy Soc. Gen. Meeting*, Detroit, MI, USA, Jul. 2011, pp. 1–8.
[40] T. Jimichi, M. Kaymak, and R. W. De Doncker, "Design and experimental verification of a three-phase dual-active bridge converter for offshore wind turbines," in *Proc. Int. Power Electron. Conf. (IPEC-Niigata -ECCE Asia)*, Niigata, Japan, May 2018, pp. 3729–3733.
[41] J. Li, B. Zhao, Q. Song, Y. Huang, and W. Liu, "DC voltage balance control strategy of high frequency link DC transformer in DC distribution system," *Proc. CSEE*, vol. 36, no. 2, pp. 327–334, 2016.
[42] S. Du, C. Zhao, M. Feng, and H. Tang, "Single-phase hybrid MMC DC transformer and its control strategy for all-DC offshore wind power system," *High Voltage Eng.*, vol. 49, no. 1, pp. 51–60, 2023.
[43] S. Xue, H. Gao, Y. Guo, and B. Xu, "Bi-level distributed active power control for a large-scale wind farm," *Power Syst. Protection Control*, vol. 49, no. 3, pp. 1–9, 2021.
[44] M. Azab, "High performance decoupled active and reactive power control for three-phase grid-tied inverters using model predictive control," *Protection Control Modern Power Syst.*, vol. 6, no. 1, pp. 1–19, Dec. 2021.
[45] H. Zhang, M. M. Belhaouane, F. Colas, R. Kadri, F. Gruson, and X. Guillaud, "On comprehensive description and analysis of MMC control design: Simulation and experimental study," *IEEE Trans. Power Del.*, vol. 36, no. 1, pp. 244–253, Feb. 2021.
[46] Q. Huang, G. Zou, L. Gao, and C. Sun, "Review on DC transmission line protection technologies of HB-MMC based DC grids," *Power Syst. Technol.*, vol. 42, no. 9, pp. 2830–2840, 2018.
[47] M. Muniappan, "A comprehensive review of DC fault protection methods in HVDC transmission systems," *Protection Control Modern Power Syst.*, vol. 6, no. 1, pp. 1–20, Dec. 2021.
[48] M. Kong, G. Tang, and Z. He, "A DC fault ride-through strategy for cell-hybrid modular multilevel converter based HVDC transmission systems," *Proc. CSEE*, vol. 34, no. 30, pp. 5343–5351, 2014.
[49] S. Deng, N. Zhou, Y. Wang, R. Lian, and L. Ran, "Research on DC fault isolation voltage based on proportions of full bridge sub-modules of hybrid MMC," *High Voltage Eng.*, vol. 44, no. 10, pp. 3250–3257, 2018.
[50] X. Wang, Z. Li, H. Wang, and Z. Yang, "Design and research of a series all-DC power generation system based on a new DC wind turbine," *Power Syst. Protection Control*, vol. 50, no. 20, pp. 178–187, 2022.
[51] H. Cui, X. Li, S. Huang, L. Huang, F. Sheng, S. Huang, D. Luo, and G. Wu, "Voltage coordinated control strategy for modular multi-phase PMSG-based series-parallel DC connected offshore wind farm," *Trans. China Electrotech. Soc.*, vol. 38, no. 4, pp. 925–935, 2023.
[52] M. Yang, Z. Yang, X. Cai, A. Usman, I. Seiki, and J. Zhang, "Method for realizing DC output of wind turbine based on diode rectifier," *High Voltage Eng.*, vol. 47, no. 8, pp. 2708–2720, 2021.
[53] Q. Liu, C. Hong, S. Fan, Z. Yuan, and X. Tian, "One kind of large-scale DC wind turbine and its control technology based on dual phase-shift power conversion," *Proc. CSEE*, vol. 43, no. 2, pp. 507–519, 2023.
[54] C. Hong, Q. Liu, Y. Liu, S. Fan, X. Tian, and Z. Yuan, "Dual three-level soft switching converter for DC grid-connected of large-scaled wind turbines," *Power Syst. Technol.*, vol. 47, no. 5, pp. 2108–2120, 2023.
[55] T. Zheng, Y. Piao, Y. Guo, and L. Yang, "Fault ride-through of bipolar short-circuit fault on output side of DC transformer," *Power Syst. Technol.*, vol. 46, no. 8, pp. 3115–3122, 2022.
[56] Y. Sun, Y. Lu, Y. Liu, Z. Wang, G. Li, and X. Wu, "Coordinated control strategy of DC fault ride-through for flexible DC grid-connected system of wind power based on energy storage," *Automat. Electr. Power Syst.*, vol. 47, no. 3, pp. 122–132, 2023.

HAIYANG HAN received the B.S. degree in electrical engineering from the Hebei University of Engineering, Handan, China, in 2020. He is currently pursuing the master's degree with the College of Electrical Engineering, Xinjiang University. His research interests include renewable energy generation, grid-connection technology, and all-dc wind power system design.

ZHANLONG LI received the M.S. degree in power electronics and power transmission from Beijing Jiaotong University, Beijing, China, in 2007. He is currently a Systems Engineer with Beijing Goldwind Science and Creation Wind Power Equipment Company Ltd., China. His research interests include flexible dc transmission technology and dc wind turbine control and networking technology.

HAIYUN WANG received the B.S. degree from the Department of Electrical Engineering, Xinjiang University, in 1995, and the M.S. degree in electrical engineering from the Dalian University of Technology, in 1996. She is a Professor with the Department of Electrical Engineering, Xinjiang University. Her research interests include the renewable energy generation and grid-connection technology, wind power dc transmission technology, new power system construction and performance analysis, big data analysis, and data processing technology.

QITA FENG received the M.S. degree in power electronics and power transmission from the Harbin University of Science and Technology, Harbin, China, in 2010. Currently, he is a Control System Engineer with Beijing Goldwind Science and Creation Wind Power Equipment Company Ltd. His research interests include wind power generation technology and HVDC transmission technology.

RUI GUO received the M.S. degree in mechanical and electronic engineering from Xi'an Jiaotong University, Xi'an, China, in 2008. He is currently a Senior Engineer with the Research and Development Center, Beijing Goldwind Science and Creation Wind Power Equipment Company Ltd., China. His research interests include new energy generation and grid-connection technology.

ZHIQIAN YANG received the M.S. degree in mechanical engineering from the Beijing Institute of Technology, Beijing, China, in 2006. He is currently a Senior Engineer with the Research and Development Center, Beijing Goldwind Science and Creation Wind Power Equipment Company Ltd., China. His research interests include new energy grid connection; power electronics technology; and the technology of power generation, transmission, loading, and storage.

XIANGPING LIU received the B.S. degree in electronic information engineering from the Beijing University of Technology, Beijing, China, in 2017. She is currently a Senior Electrical Engineer with the Research and Development Center, Beijing Goldwind Science and Creation Wind Power Equipment Company Ltd., China. Her research interests include medium and high voltage electrical technology and flexible dc power transmission and transformation technology.